Monopoles and Quark Confinement

Tsuneo SUZUKI

Department of Physics, Kanazawa University, Kanazawa 920-11, Japan

I review the studies of quark confinement based on the dual Meissner effect due to monopole condensation after abelian projection in QCD. The first part is about Monte Carlo simulations of abelian projection and the role of monopoles in lattice QCD. Abelian projection in the maximally abelian gauge is found very interesting. The monopole part alone is responsible for confinement. A block spin transformation on the dual lattice and energy-entropy balance of the monopole loops suggest that lattice $SU(2)$ QCD is always (for all β) in the monopole condensed phase and so in the confinement phase in the infinite volume limit. Abelian Polyakov loops in various gauges suggest gauge independence of the picture of the monopole condensation. The effective field theory composed of a dual photon and a monopole field based on the monopole condensation after abelian projection is shortly reviewed in the next part.

§ 1. Introduction

It has been evident from Monte Carlo simulations of lattice QCD that quarks are confined. However why and how quarks are confined is not yet known. It is crucial to understand the mechanism of quark confinement in order to explain hadron physics out of QCD. The 't Hooft idea of abelian projection of QCD is interesting.[1] The abelian projection is to fix the gauge in such a way that the maximal torus group remains unbroken. After the abelian projection, monopoles appear as a topological quantity in the residual abelian channel. QCD is reduced to an abelian theory with electric charges and monopoles. If the monopoles make Bose condensation, charged quarks and gluons are confined due to the dual Meissner effect. Namely, color confinement can be regarded as abelian charge confinement caused by the monopole condensation.

On the basis of this standpoint, the present author and his collaborators have studied color confinement mechanism and hadron physics adopting two approaches. The first approach is Monte Carlo simulations of abelian projection in lattice QCD.[2)~13)] The aim of the study is to ascertain correctness of the picture, that is, to check if monopole condensation really occurs and if it is the confinement mechanism in QCD. The second approach is to construct an infrared effective Lagrangian directly from QCD on the assumption of the above picture and to explain low energy hadron physics from the effective theory.[14)~18)] The purpose of this report is to review the results of these studies compactly.

In the next section, what is abelian projection is shortly explained. Section 3 reviews the results of the Monte Carlo simulations of abelian projection. Section 4

is the short summary of the studies based on the infrared effective theory of QCD. Final section is devoted to concluding remarks.

§ 2. Abelian projection

2.1. *Abelian projection in the continuum QCD*

Abelian projection of QCD is done as follows. Choose an operator $X(x)$ which is transformed non-trivially under $SU(3)$ transformation:

$$A_\mu(x) \to \tilde{A}_\mu(x) = V(x)A_\mu(x)V^\dagger(x) - \frac{i}{g}\partial_\mu V(x)V^\dagger(x), \tag{1}$$

$$\psi(x) \to \tilde{\psi}(x) = V(x)\psi(x). \tag{2}$$

Abelian projection is to choose $V(x)$ so that $X(x)$ is diagonalized as

$$X(x) \to \tilde{X}(x) = \begin{pmatrix} \lambda_1(x) & & \\ & \lambda_2(x) & \\ & & \lambda_3(x) \end{pmatrix}. \tag{3}$$

$V(x)$ is fixed up to the diagonal element $d(x)$ of $SU(3)$, where

$$d(x) = \begin{pmatrix} \exp(i\alpha_1(x)) & & \\ & \exp(i\alpha_2(x)) & \\ & & \exp(i\alpha_3(x)) \end{pmatrix} \in SU(3), \quad \sum_{i=1}^{3}\alpha_i(x) = 0. \tag{4}$$

$\{d(x)\}$ is the maximum torus group of $SU(3)$, which is the residual $U(1)\times U(1)$ gauge symmetry.

We look at QCD at this stage without further fixing the gauge of the residual symmetry. First, we explore how the fields after the abelian projection transform *under an arbitrary SU(3) gauge transformation* $W(x)$. Since $X(x)$ is a functional of (gauge) fields and so it transforms under $W(x)$. Hence $V(x)$ also transforms non-trivially. Let us fix the form of $V(x)$ such that all diagonal components of the exponent of $V(x)$ are zero. This is always possible if one uses the residual symmetry. Then $V(x)$ is found to transform *under* $W(x)$ as

$$V(x) \xrightarrow{W} V^W(x) = d^W(x)V(x)W^\dagger(x). \tag{5}$$

$V^W(x)$ diagonalizes an operator which is transformed from $X(x)$ under $W(x)$. $d^W(x)$ is necessary for $V^W(x)$ to take the fixed form.

The gauge field after the abelian projection, $\tilde{A}_\mu(x)$, transforms *under* $W(x)$ as

$$\tilde{A}_\mu(x) \xrightarrow{W} \tilde{A}_\mu{}^W(x) = d^W(x)\tilde{A}_\mu(x)d^{W\dagger}(x) - \frac{i}{g}\partial_\mu d^W(x)d^{W\dagger}(x). \tag{6}$$

After the abelian projection, $\tilde{A}_\mu(x)$ transforms only under the diagonal matrix $d^W(x)$. Since the last term of (6) is composed of the diagonal part alone, the diagonal part of $\tilde{A}_\mu(x)$ transforms like a photon. The off diagonal part of $\tilde{A}_\mu(x)$ transforms like a charged matter. The quark field transforms *under* $W(x)$ as

$$\tilde{\psi}(x) \xrightarrow{W} \tilde{\psi}^W(x) = d^W(x)\tilde{\psi}(x). \tag{7}$$

It is important that $\tilde{\phi}_i^\dagger(x)\tilde{\phi}_i(x)$*) and $\tilde{\phi}_1(x)\tilde{\phi}_2(x)\tilde{\phi}_3(x)$ are neutral and at the same time invariant under any $SU(3)$ transformation $W(x)$. *Color confinement is regarded as abelian charge confinement after abelian projection.*

The most interesting fact of abelian projection is that monopoles appear in the residual abelian channel. We treat $SU(2)$ QCD for simplicity. After abelian projection, we define an abelian field strength as

$$f_{\mu\nu}(x)=\partial_\mu \tilde{A}_\nu{}^3(x)-\partial_\nu \tilde{A}_\mu{}^3(x)\,. \tag{8}$$

The abelian field $\tilde{A}_\mu{}^3(x)$ written in terms of the original field is

$$\tilde{A}_\mu{}^3(x)=\hat{Y}^a(x)A_\mu{}^a(x)-\frac{1}{g}\frac{1}{1+\hat{Y}^3(x)}\epsilon_{3ab}\hat{Y}^a(x)\partial_\mu\hat{Y}^b(x)\,, \tag{9}$$

where $\hat{Y}(x)=V^\dagger(x)\sigma_3 V(x)=\hat{Y}^a(x)\sigma^a\cdot\hat{Y}^a(x)$ obeys

$$\hat{Y}^a(x)\hat{Y}^a(x)=1\,. \tag{10}$$

$f_{\mu\nu}(x)$ can be rewritten in the form

$$f_{\mu\nu}(x)=\partial_\mu(\hat{Y}^a(x)A_\nu{}^a(x))-\partial_\nu(\hat{Y}^a(x)A_\mu{}^a(x))-\frac{1}{g}\epsilon_{abc}\hat{Y}^a(x)\partial_\mu\hat{Y}^b(x)\partial_\nu\hat{Y}^c(x) \tag{11}$$

in terms of the original field. A current

$$k_\mu(x)=\frac{1}{2}\epsilon_{\mu\nu\rho\sigma}\partial^\nu f^{\rho\sigma}(x)\,, \tag{12}$$

$$=\frac{1}{2g}\epsilon_{\mu\nu\rho\sigma}\epsilon_{abc}\partial^\nu\hat{Y}^a(x)\partial^\rho\hat{Y}^b(x)\partial^\sigma\hat{Y}^c(x) \tag{13}$$

is always zero if $V(x)$ is fixed. However, at a point x where the eigenvalue of the diagonalized operator $X(x)$ is degenerate, $V(x)$ is not well defined and $k_\mu(x)$ does not vanish there. We calculate the charge in the three dimensional volume Ω around x:[19]

$$g_m=\int_\Omega k_0(x)d^3x=\frac{1}{2g}\int_\Omega\epsilon_{0\nu\rho\sigma}\epsilon_{abc}\partial^\nu\hat{Y}^a(x)\partial^\rho\hat{Y}^b(x)\partial^\sigma\hat{Y}^c(x)d^3x\,, \tag{14}$$

$$=\frac{1}{2g}\int_{\partial\Omega}\epsilon_{ijk}\epsilon_{abc}\hat{Y}^a(x)\partial_j\hat{Y}^b(x)\partial_k\hat{Y}^c(x)d^2\sigma_i\,, \tag{15}$$

$$=\frac{4\pi n}{g}\,, \tag{16}$$

where n is an integer. n is a topological number corresponding to a mapping between the sphere (10) in the parameter space and the sphere $\partial\Omega$ of Ω. Because this equation represents the Dirac quantization condition, g_m can be interpreted as a magnetic charge. The monopole current $k_\mu(x)$ is a topologically conserved current $\partial_\mu k^\mu(x)=0$. *Abelian projected QCD can be regarded as an abelian theory with electric*

*) Each $\tilde{\phi}_i^\dagger(x)\tilde{\phi}_i(x)$ $(i=1\sim3)$ is $SU(3)$ invariant. The sum $\sum_i^3\tilde{\phi}_i^\dagger(x)\tilde{\phi}_i(x)$ is the lowest color singlet as seen from $\sum_i^3\tilde{\phi}_i^\dagger(x)\tilde{\phi}_i(x)=\sum_i^3\psi_i^\dagger(x)\psi_i(x)$. Other two are excited singlet states composed of quarks and gluons.

charges and monopoles. 't Hooft[1] conjectured if the monopoles condense, abelian charges are confined due to the dual Meissner effect. This means color confinement.

2.2. *Abelian projection on a lattice*

We can perform abelian projection on a lattice similarly. Choose an operator $X(s)$ in, for simplicity, $SU(2)$ QCD. The gauge transformation on a lattice is

$$\tilde{U}(s, \hat{\mu}) = V(s) U(s, \hat{\mu}) V^{\dagger}(s+\hat{\mu}) , \tag{17}$$

where $U(s, \hat{\mu})$ represents a link field corresponding to a gauge field in the continuum theory. After abelian projection is over, abelian link fields can be separated from $SU(2)$ link fields as follows:

$$\tilde{U}(s, \hat{\mu}) = \begin{pmatrix} \sqrt{1-|c(s,\mu)|^2} & -c^*(s,\mu) \\ c(s,\mu) & \sqrt{1-|c(s,\mu)|^2} \end{pmatrix} \begin{pmatrix} e^{i\theta_\mu(s)} & 0 \\ 0 & e^{-i\theta_\mu(s)} \end{pmatrix}, \tag{18}$$

$$= C(s, \hat{\mu}) u(s, \hat{\mu}) . \tag{19}$$

$u(s, \hat{\mu})$ transforms like a photon and $C(s, \hat{\mu})$ transforms like a charged matter under the residual $U(1)$ gauge symmetry. The abelian field strength is defined as a plaquette variable

$$\theta_{\mu\nu}(s) = \theta_\mu(s) + \theta_\nu(s+\hat{\mu}) - \theta_\mu(s+\hat{\nu}) - \theta_\nu(s) . \tag{20}$$

The monopole current is defined[20] as

$$k_\mu(s) = \frac{1}{2} \epsilon_{\mu\nu\rho\sigma} \partial_\nu n_{\rho\sigma}(s+\hat{\mu}) , \tag{21}$$

where ∂_ν is a forward derivative on a lattice and $\theta_{\mu\nu}(s)$ is decomposed into

$$\theta_{\mu\nu}(s) = \bar{\theta}_{\mu\nu}(s) + 2\pi n_{\mu\nu}(s) , \quad -\pi < \bar{\theta}_{\mu\nu}(s) \leq \pi . \tag{22}$$

$n_{\mu\nu}(s)$ is an integer corresponding to the number of the Dirac string through the plaquette. The monopole currents are conserved topologically

$$\partial'_\mu k_\mu = 0 , \tag{23}$$

where ∂'_μ is a backward derivative on a lattice. The monopole currents make closed loops on the four dimensional lattice.

§ 3. Monte Carlo study of abelian projection in lattice QCD

Our procedure is as follows:

1. Vacuum configurations of link variables $\{U(s, \mu)\}$ are generated with the Wilson action.
2. We perform an abelian projection and then separate abelian link variables $u(s, \mu)$ as in (19) to obtain an ensemble of $\{u(s, \mu)\}$.
3. We construct monopole curents following the DeGrand-Toussaint method as in (21).[20]

4. We measure expectation values of $U(1)\times U(1)$ invariant operators $O(u(s,\mu))$ and operators composed of monopole currents $O(k_\mu(s))$.

3.1. *Abelian dominance in MA gauge*

There are infinite ways of abelian projection extracting such an abelian theory out of QCD. It seems important to find a good gauge at least in the studies on a small lattice. I show in the following, if one adopts a gauge called maximally abelian gauge,[21),2),3)] the 't Hooft conjecture is beautifully realized at least in $SU(2)$ QCD.

Define a matrix

$$X(s)=\sum_\mu[U(s,\mu)\sigma_3 U^\dagger(s,\mu)+U^\dagger(s-\mu,\mu)\sigma_3 U(s-\mu,\mu)]$$

$$=X_1(s)\sigma_1+X_2(s)\sigma_2+X_3(s)\sigma_3\,.$$

Then a gauge satisfying $X_1(s)=X_2(s)=0$ is the maximally abelian gauge which tends to a $U(1)$-convariant gauge $(\partial_\mu\pm igA_\mu^3)A^{\pm\mu}=0$ in the continuum limit.

Gauge-fixed link variables are decomposed into a product of two matrices as above. We have found that abelian loop operators composed of $u(s,\mu)$ alone seem to reproduce essential features of QCD color confinement in MA gauge.[2),3)] Explicitly, abelian static potentials derived from abelian Wilson loops composed of $u(s,\mu)$ alone is plotted in Fig. 1 of Ref. 2) in comparison with full ones.[2)] The string tensions are derived from the static potentials. The abelian and the full string tensions are about the same.

Polyakov loops and energy densities play the role of an order parameter of the deconfinement transition in finite-temperature pure QCD also in the abelian case.[3)] The abelian quantities show clearer behaviors around the critical coupling.

3.2. *Effective U(1) action*

The above abelian dominance suggests that a set of $U(1)$ invariant operators $\{O(u(s,\mu))\}$ are enough to describe confinement. Then there must exist an effective $U(1)$ action $S_{\rm eff}(u)$ describing confinement. These matrix elements are obtained as follows:

$$\langle O(u)\rangle=\frac{\int e^{-S(U)}\delta(X^\pm)\Delta_F(U)O(u)DU}{\int e^{-S(U)}\delta(X^\pm)\Delta_F(U)DU}$$

$$=\frac{\int DuO(u)\left[\int DCe^{-S(u,C)}\delta(X^\pm)\Delta_F(U)\right]}{\int Du\left[\int DCe^{-S(u,C)}\delta(X^\pm)\Delta_F(U)\right]}$$

$$=\frac{\int Due^{-S_{\rm eff}(u)}O(u)}{\int Due^{-S_{\rm eff}(u)}}\,.$$

We tried to derive $S_{\rm eff}(u)$ using Schwinger-Dyson equations, but failed to get it in a compact and local form.[3)] $S_{\rm eff}(u)$ contains larger and larger loops as β.

3.3. *Effective monopole U(1) action $S(k_\mu(s))$*

In compact QED with the Villain action,[22] one can perform a dual transformation analytically to obtain an effective action expressed in terms of monopole currents. Shiba and the present author tried to perform a dual transformation of $S_{\text{eff}}(u)$ in $SU(2)$ QCD and to obtain the effective $U(1)$ action in terms of monopole currents.[4),7),11)] The above monopole current is defined by $n_{\mu\nu}(s)$ surrounding the smallest cube as shown in (21). To study the long range behavior important in QCD, we considered extended monopoles.[23] They are defined by $n_{\mu\nu}(s)$ surrounding an extended cube:

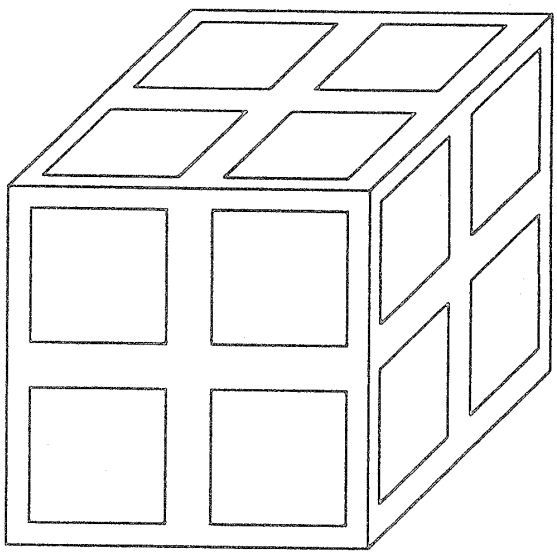

Fig. 1. An extended cube on which a 2^3 extended monopole is defined as the sum of eight ($=2^3$) smallest monopoles.

$$k_\mu{}^{(n)}(s)=\frac{1}{2}\epsilon_{\mu\nu\rho\sigma}\partial_\nu m_{\rho\sigma}^{(n)}(s+\hat{\mu})\,, \tag{24}$$

$$=\sum_{i,j,l=0}^{n-1} k_\mu(ns+(n-1)\hat{\mu}+i\hat{\nu}+j\hat{\rho}+l\hat{\sigma})\,, \tag{25}$$

$$m_{\rho\sigma}^{(n)}(s)=\sum_{i,j=0}^{n-1} m_{\rho\sigma}(ns+i\hat{\rho}+j\hat{\sigma})\,. \tag{26}$$

For example, Fig. 1 represents a 2^3 cube defining a 2^3 extended monopole. Adopting an n^3 extended monopole corresponds to performing a block spin transformation on a dual lattice[7),11)] and so is suitable for exploring the long range property of QCD. Note for example that

$$k_\mu{}^{(4)}(s)=\sum_{i,j,l=0}^{3} k_\mu(4s+3\hat{\mu}+i\hat{\nu}+j\hat{\rho}+l\hat{\sigma})$$

$$=\sum_{i,j,l=0}^{1} k_\mu{}^{(2)}(2s+\hat{\mu}+i\hat{\nu}+j\hat{\rho}+l\hat{\sigma})\,, \tag{27}$$

$$k_\mu{}^{(2)}(s)=\sum_{i,j,l=0}^{1} k_\mu(2s+\hat{\mu}+i\hat{\nu}+j\hat{\rho}+l\hat{\sigma})\,. \tag{28}$$

When adopting an n^3 extended monopole on $N_s{}^3\times N_t$ lattice, the effective lattice (which we call a renormalized lattice) on which the extended monopole runs is

$$\left(\frac{N_s}{n}\right)^3\times\left(\frac{N_t}{n}\right). \tag{29}$$

Hence the following is an example of a block spin transformation:

$$\begin{pmatrix} k_\mu(s) \\ a \\ N^4 \end{pmatrix} \longrightarrow \begin{pmatrix} k_\mu^{(2)}(s) \\ 2a \\ (N/2)^4 \end{pmatrix} \longrightarrow \begin{pmatrix} k_\mu^{(4)}(s) \\ 4a \\ (N/4)^4 \end{pmatrix} \longrightarrow \cdots . \tag{30}$$

The partition function of interacting monopole currents is expressed as

$$Z=(\prod_{s,\mu} \sum_{k_\mu(s)=-\infty}^{\infty})(\prod_s \delta_{\partial'_\mu k_\mu(s),0})\exp(-S[k]) . \tag{31}$$

It is natural to assume $S[k]=\sum_i f_i S_i[k]$. Here f_i is a coupling constant of an interaction $S_i[k]$. For example, f_1 is the coupling of the self-energy term $\sum_{s,\mu}(k_\mu(s))^2$, f_2 is the coupling of a nearest-neighbor interaction term $\sum_{s,\mu} k_\mu(s)k_\mu(s+\hat{\mu})$ and f_3 is the coupling of another nearest-neighbor term $\sum_{s,\mu\neq\nu} k_\mu(s)k_\mu(s+\hat{\nu})$.[7] Shiba and Suzuki[4),6),7)] extended a method developed by Swendsen[24)] to the system of monopole currents obeying the current conservation rule (23).

The monopole actions are obtained locally enough for all extended monopoles considered even in the scaling region as shown in Fig. 2. They are lattice volume independent. The coupling constant f_1 of the self-energy term is dominant and the coupling constants decrease rapidly as the distance between the two monopole currents increases.

Since the action is fixed, it is possible to study energy and entropy balance of monopole loops in order to confirm the occurrence of monopole condensation. If the entropy of a monopole loop exceeds the energy, the condensation of a monopole loop occurs. As done in compact QED,[25)] the entropy of a monopole loop can be estimated as ln 7 per unit loop length. Since monopole currents are distributed randomly in average for large L, interaction terms between two separate currents are seen to be cancelled.[13)] Hence the action is approximated by the self-energy part $f_1 L$. Since f_1 is regarded as the self-energy per unit monopole loop length, the free energy per unit

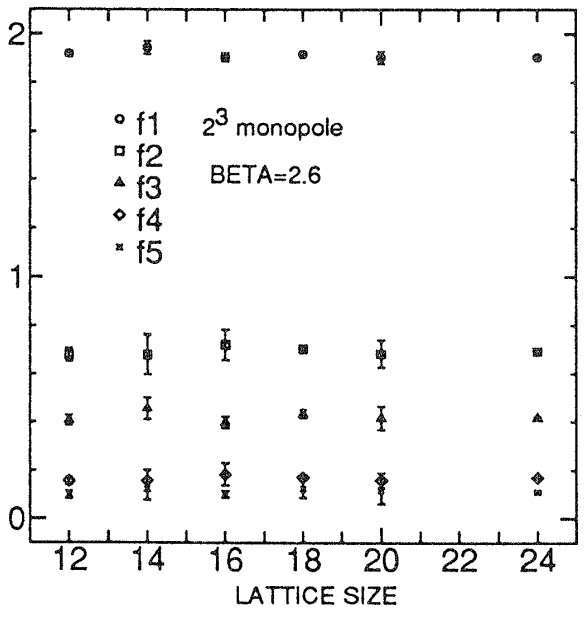

Fig. 2. Coupling constants f_i versus lattice size.

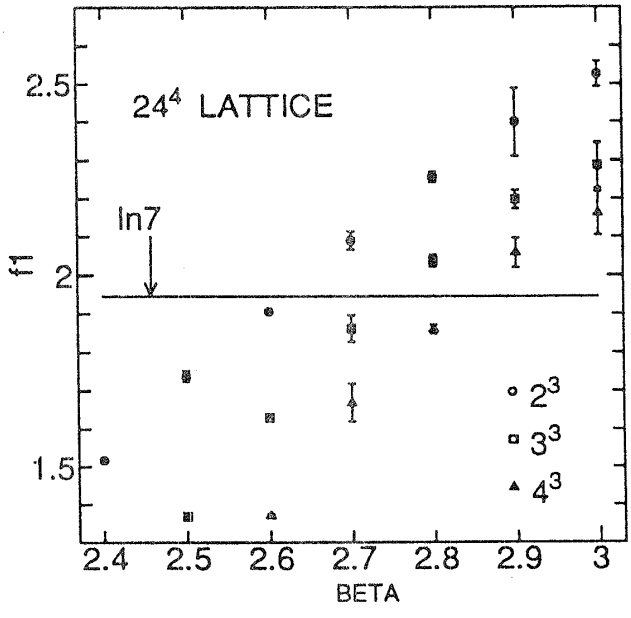

Fig. 3. Coupling constants f_1 versus β for 2^3, 3^3, and 4^3 extended monopoles on 24^4 lattice.

monopole loop length is approximated by $(f_1-\ln 7)$. If $f_1<\ln 7$, the entropy dominates over the energy, which means condensation of monopoles. In Fig. 3, f_1 versus β for various extended monopoles on 24^4 lattice is shown in comparison with the entropy value $\ln 7$. Each extended monopole has its own β region where the condition $f_1<\ln 7$ is satisfied. When the extendedness is bigger, larger β is included in such a region. Larger extended monopoles are more important in determining the phase transition point.

The behaviors of the coupling constants are different for different extended monopoles. However, if we plot them versus $b=n\times a(\beta)$, we get a unique curve as in Fig. 4. The coupling constants seem to depend only on b, not on the extendedness nor β. There is a critical b_c corresponding to critical β_c^n, i.e., $b_c=na(\beta_c^n)$. The monopole action may be fitted by

$$S[k]=\sum m_0 b k_\mu(s)k_\mu(s)+\frac{1}{2}\left(\frac{4\pi}{g(b)}\right)^2\sum k_\mu(s)\bar{D}(s-s')k_\mu(s')\,, \tag{32}$$

where $g(b)$ is the $SU(2)$ running coupling constant

$$g(b)^{-2}=\frac{11}{24\pi^2}\ln\left(\frac{1}{b^2\Lambda^2}\right)+\frac{17}{44\pi^2}\ln\ln\left(\frac{1}{b^2\Lambda^2}\right). \tag{33}$$

$\bar{D}(s)$ is a modified lattice Coulomb propagator. This form of the action is predicted theoretically by Smit and Sijs.[26] The solid line is the prediction given by the action with the parameters written in Fig. 4.

Now we can derive important conclusions. Suppose the effective monopole action remains the same for any extended monopoles larger than 4^3 in the infinite volume limit. Then the finiteness of $b_c=na(\beta_c^n)$ suggests β_c^n becomes infinite when the extendedness n goes to infinity. $SU(2)$ lattice QCD is always (for all β) in the monopole condensed and then in the color confinement phase.[1] This is one of what one wants to prove in the framework of lattice QCD.

Notice again that considering extended monopoles correspond to performing a block spin transformation on the dual lattice. The above fact that the effective actions for all extended monopoles considered are the same for fixed b means that the action may be the renormalized trajectory on which one can take the continuum limit. Our results suggest the continuum monopole action takes the form (32) predicted by Smit and Sijs.[26] The simulation of the monopole action is in progress.

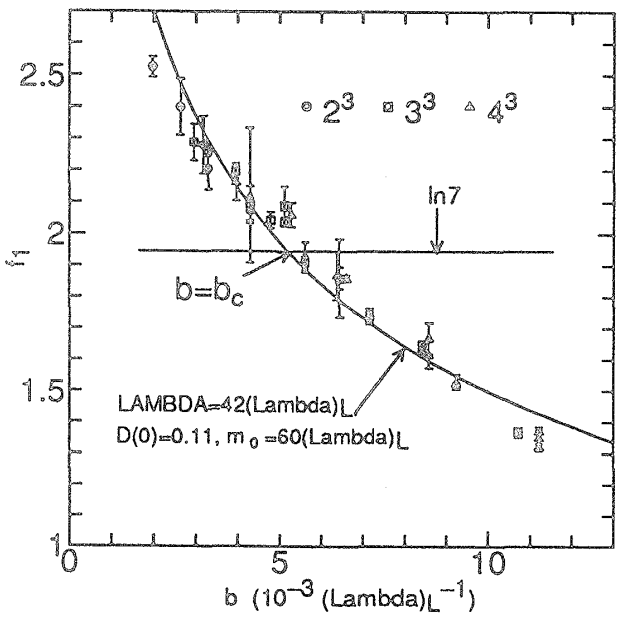

Fig. 4. Coupling constants f_1 and f_2 versus b.

3.4. *The string tension and monopoles*

Shiba and Suzuki[4),5)] have shown

furthermore that monopoles alone can reproduce the full value of the string tension in $SU(2)$ QCD. Let us show an abelian Wilson loop operator is rewritten by a product of monopole and photon contributions. Here we take into account only a simple Wilson loop, say, of size $I\times J$. Then such an abelian Wilson loop operator is expressed as

$$W=\exp\{i\sum J_\mu(s)\theta_\mu(s)\}\,, \tag{34}$$

where $J_\mu(s)$ is an external current taking ±1 along the Wilson loop. Since $J_\mu(s)$ is conserved, it is rewritten for such a simple Wilson loop in terms of an antisymmetric variable $M_{\mu\nu}(s)$ as $J_\nu(s)=\partial'_\mu M_{\mu\nu}(s)$. $M_{\mu\nu}(s)$ takes ±1 on a surface with the Wilson loop boundary. Although we can choose any surface of such a type, we adopt a minimal surface here. We get

$$W=\exp\left\{-\frac{i}{2}\sum M_{\mu\nu}(s)\theta_{\mu\nu}(s)\right\}. \tag{35}$$

The gauge plaquette variable can be decomposed into $\theta_{\mu\nu}(s)=\bar{\theta}_{\mu\nu}(s)+2\pi n_{\mu\nu}(s)$ as (22). Since $M_{\mu\nu}(s)$ and $n_{\mu\nu}(s)$ are integers, the latter does not contribute to Eq. (35). Hence $\theta_{\mu\nu}(s)$ in Eq. (35) is replaced by $\bar{\theta}_{\mu\nu}(s)$. Using a decomposition rule

$$M_{\mu\nu}(s)=-\sum D(s-s')\left[\partial'_\alpha(\partial_\mu M_{\alpha\nu}-\partial_\nu M_{\alpha\mu})(s')+\frac{1}{2}\epsilon_{\alpha\beta\mu\nu}\epsilon_{\alpha'\beta\rho\sigma}\partial'_\alpha\partial'_{\alpha'}M_{\rho\sigma}(s')\right],$$

we get

$$W=W_1\cdot W_2\,,$$

$$W_1=\exp\{-i\sum\partial'_\mu\bar{\theta}_{\mu\nu}(s)D(s-s')J_\nu(s')\}$$

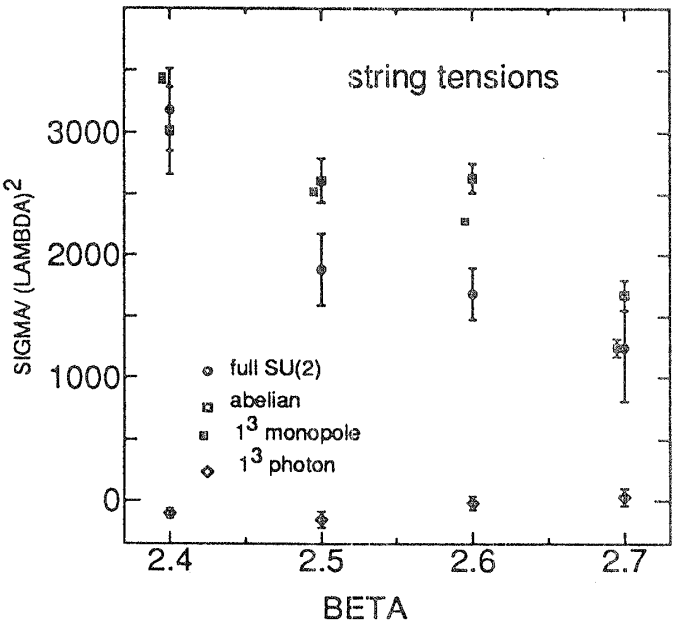

Fig. 5. String tensions from monopoles (cross) and photons (diamond) in comparison with those from abelian (circle) and full (square) Wilson loops on 24^4 lattice.

$$W_2=\exp\left\{2\pi i\sum k_\beta(s)D(s-s')\frac{1}{2}\epsilon_{\alpha\beta\rho\sigma}\partial_\alpha M_{\rho\sigma}(s')\right\}. \tag{36}$$

$D(s)$ is the lattice Coulomb propagator. Since $\partial'_\mu\bar{\theta}_{\mu\nu}(s)$ contains only the photon field, $W_1(W_2)$ is the photon (the monopole) contribution to the Wilson loop. To study the features of both contributions, we evaluate the expectation values $\langle W_1\rangle$ and $\langle W_2\rangle$ separately and compare them with those of W. The string tensions evaluated from monopole and photon contributions are plotted in Fig. 5. The string tension is reproduced only from the monopole contribution.

3.5. *Polyakov loops and monopoles*

An abelian Polyakov loop P which is written in terms of abelian link fields alone

$$P=\mathrm{Re}[\exp\{i\sum_{i=1}^{N_4}J_4(s+(i-1)\hat{4})\theta_4(s+(i-1)\hat{4})\}] \tag{37}$$

is given by a product of contributions from Dirac strings of monopoles and from photons. Here $J_4(s)$ is an external current taking $+1$ along the straight line in the fourth direction. Using the definition of a plaquette variable $\theta_{\mu\nu}(s)=\partial_\mu\theta_\nu(s)-\partial_\nu\theta_\mu(s)$ where ∂_μ is a forward difference, we get

$$\theta_4(s)=-\sum_{s'}D(s-s')[\partial'_\nu\theta_{\nu4}(s')+\partial_4(\partial'_\nu\theta_\nu(s'))]. \tag{38}$$

Since $\partial'_4J_4(s)=0$, the second term on the right-hand side of (38) does not contribute to the abelian Polyakov loop (37). Hence we get

$$P=\mathrm{Re}[\exp\{-i\sum_{i=1}^{N_4}J_4(s+(i-1)\hat{4})\sum_{s'}D(s+(i-1)\hat{4}-s')\partial'_\nu\theta_{\nu4}(s')\}]. \tag{39}$$

We get

$$P=\mathrm{Re}[P_1\cdot P_2], \tag{40}$$

$$P_1=\exp\{-i\sum_{i=1}^{N_4}J_4(s+(i-1)\hat{4})\sum_{s'}D(s+(i-1)\hat{4}-s')\partial'_\nu\bar{\theta}_{\nu4}(s')\}, \tag{41}$$

$$P_2=\exp\{-2\pi i\sum_{i=1}^{N_4}J_4(s+(i-1)\hat{4})\sum_{s'}D(s+(i-1)\hat{4}-s')\partial'_\nu n_{\nu4}(s')\}. \tag{42}$$

We observe the photon (P_p) and the Dirac-string (P_m) contributions separately:

$$P_p=\mathrm{Re}[P_1]\quad\text{and}\quad P_m=\mathrm{Re}[P_2]. \tag{43}$$

It has been found[10),12)] that the characteristic features of the Polyakov loops as an order parameter of the deconfinement transition are due to the Dirac string contributions alone. In Fig. 6, the $SU(2)$ data in MA gauge are plotted. The abelian Polyakov loops vanish in the confinement phase whereas they begin to rise for β larger than the critical temperature $\beta_c=2.298$. The Dirac string contribution shows similar behaviors more drastically. The photon part has a finite contribution for both phases and it changes only slightly. The fact that monopoles are responsible for the essential feature of the Polyakov loop is found also in $U(1)$ and in $SU(3)$ in MA gauge.

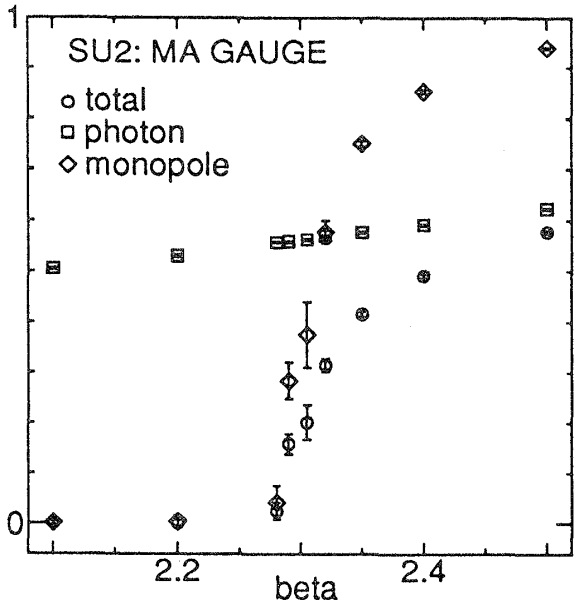

Fig. 6. Monopole Dirac string and photon contributions to Polyakov loops in MA gauge in $SU(2)$ QCD on $16^3\times4$ lattice. Total means the abelian Poyakov loops.

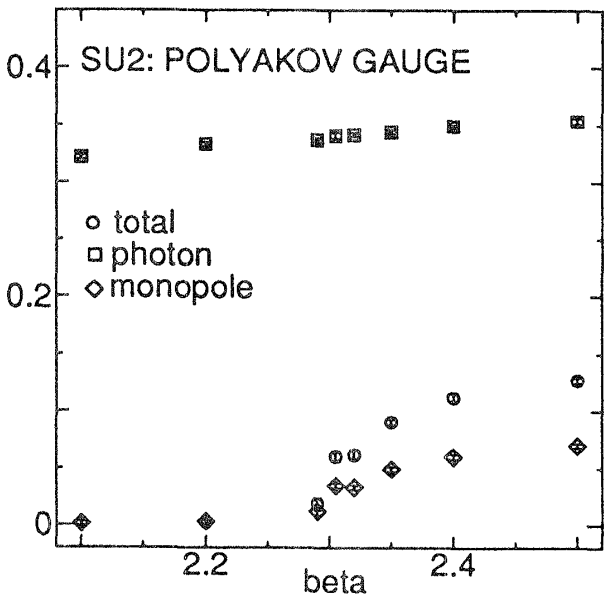

Fig. 7. Monopole Dirac string and photon contributions to Polyakov loops in the Polyakov gauge.

In addition, a remarkable result has been found. The behavior of the abelian Polyakov loops as an order parameter and the monopole responsibility are seen also *in other gauges like unitary ones*.[10] See Fig. 7. This is the first phenomenon suggesting gauge independence of the 't Hooft conjecture.

3.6. *Summary of Monte Carlo studies of abelian projection*

1. Monopole condensation seems to be the confinement mechanism at least in MA gauge of $SU(2)$ QCD.
2. Indication of gauge independence of the picture is found.
3. Construction of the effective monopole action in $SU(3)$ QCD and in full QCD is highly expected.

§ 4. An infrared effective field theory of QCD

4.1. *Dual abelian effective theory of QCD*

The monopole action derived above may be interpreted as a monopole Coulomb gas with the running coupling constant and the bare mass. $(f_1(b)-\ln 7)$ is the free energy per unit monopole-loop length which is regarded as a chemical potential. The other interaction terms may be interpreted as a bond-bond interaction due to the Coulomb potential in the continuum limit. Using the technique developed by Samuel,[27] such a system is described by an abelian Higgs model (also see Ref. 28)):

$$S=\int d^4x\left\{\left|\partial_\mu\chi+i\frac{4\pi}{g(b)}C_\mu\chi\right|^2-\mu^2|\chi|^2-\frac{1}{4}(\partial_\mu C_\nu-\partial_\nu C_\mu)^2\right\},$$

where $\mu^2 \propto (f_1(b) - \ln 7)$ and C_μ is a dual photon. In addition, there must exist a χ^4 term which stabilizes the vacuum for $\mu^2 < 0$.

The field theoretical form of the action thus obtained is just equal to a Ginzburg-Landau type theory of confinement. I derived earlier theoretically from QCD on the assumption of abelian dominance.[14] In $SU(2)$ QCD, it is given by

$$\mathcal{L} = -\frac{1}{4} H_{\mu\nu} H^{\mu\nu} + |(\partial_\mu + igC_\mu)\chi|^2 - \lambda(|\chi|^2 - v^2)^2 , \tag{44}$$

where

$$H_{\mu\nu} = \partial_\mu C_\nu - \partial_\nu C_\mu + \epsilon_{\mu\nu\lambda\sigma} \int d^4y n^\lambda (n \cdot \partial)^{-1}(x-y) j^\sigma_{\rm ex}(y) . \tag{45}$$

Here we have introduced an external (color) electric $U(1)$ current $j^\sigma_{\rm ex}$ and g is the magnetic charge. The equations of motion are given by

$$(-\partial_i \partial_i + g^2 C_i C_i)\chi + 2\lambda(\chi^2 - v^2)\chi = 0 \tag{46}$$

and

$$-\partial_j H_{ji} + 2g^2 \chi^2 C_i = 0 . \tag{47}$$

The $SU(3)$ case is obtained as follows:

$$\mathcal{L} = -\frac{1}{4} (\mathcal{H}_{\mu\nu})^2 + \sum_{\alpha=1}^{3} \{|(\partial_\mu + ig\boldsymbol{\epsilon}_\alpha \cdot \boldsymbol{C}_\mu)\chi_\alpha|^2 - \lambda(|\chi_\alpha|^2 - v^2)^2\} , \tag{48}$$

where $\boldsymbol{\epsilon}_\alpha$ is the root vector: $\boldsymbol{\epsilon}_1 = (1, 0)$, $\boldsymbol{\epsilon}_2 = (-1/2, -\sqrt{3}/2)$ and $\boldsymbol{\epsilon}_3 = (-1/2, \sqrt{3}/2)$ and

$$\mathcal{H}_{\mu\nu} = \partial_\mu \boldsymbol{C}_\nu - \partial_\nu \boldsymbol{C}_\mu + \epsilon_{\mu\nu\lambda\sigma} \int d^4y n^\lambda (n \cdot \partial)^{-1}(x-y) \boldsymbol{j}^\sigma_{\rm ex} . \tag{49}$$

Here we have used the vector notation with respect to $U(1) \times U(1)$, e.g., $\boldsymbol{C}_\mu = (C_\mu^3, C_\mu^8)$. Adopting the unitary gauge $\mathrm{Im}(\chi_\alpha) = 0$, we have the following equations:

$$\partial_\mu \partial^\mu \chi_\alpha - g^2 (\boldsymbol{\epsilon}_\alpha \cdot \boldsymbol{C}_\mu)(\boldsymbol{\epsilon}_\alpha \cdot \boldsymbol{C}^\mu)\chi_\alpha + 2\lambda(\chi_\alpha{}^2 - v^2)\chi_\alpha = 0 . \quad (\alpha = 1, 2, 3) \tag{50}$$

$$\partial_\mu \mathcal{H}^{\mu\nu} + 2g^2 \sum_{\alpha=1}^{3} \boldsymbol{\epsilon}_\alpha (\boldsymbol{\epsilon}_\alpha \cdot \boldsymbol{C}^\nu)\chi_\alpha{}^2 = 0 . \tag{51}$$

4.2. *Applications to low energy hadron physics*

We have applied the model to various low energy hadron physics. The followings are the short review of them.

4.2.1. Static meson potential

Static meson potential is evaluated introducing an external current due to a static quark antiquark pair:[14),15]

$$j^\mu_{\rm ex}(r) = \boldsymbol{Q} g^{\mu 0} \delta(x)\delta(y)\left\{\delta\left(z - \frac{R}{2}\right) - \delta\left(z + \frac{R}{2}\right)\right\} , \tag{52}$$

where $\boldsymbol{Q} = (Q^3, Q^8) = (-e/2, -e/2\sqrt{3})$. Here e is related to g by the Dirac quantization condition $eg = 4\pi$. Solving the equation of motions (46), (47), (50) and (51), we have gotten the static meson potentials for $SU(2)$ and $SU(3)$ QCD. They are expres-

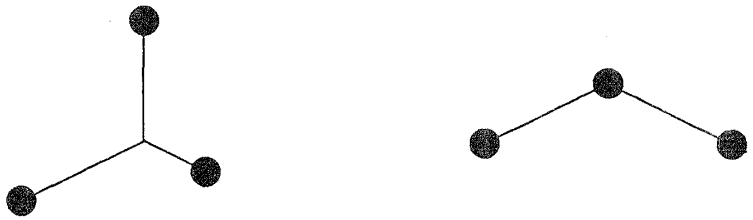

Fig. 8. Minimum string configurations.

sed as linear plus Yukawa terms:

$$V=\sigma r-\frac{\boldsymbol{Q}^2}{4\pi}\frac{e^{-mr}}{r}. \tag{53}$$

That the linear potential can be derived naturally is the promising point of the model.

4.2.2. Static baryon potential

One can evaluate a static baryon potential also by solving the equation of motions (50) and (51) with static three quark sources[17]

$$\boldsymbol{j}^{\sigma}_{\mathrm{ex}}=g^{\sigma 0}\Big\{\boldsymbol{Q}_1\delta\Big(x+\frac{\sqrt{3}}{2}R\Big)\delta\Big(y+\frac{R}{2}\Big)$$

$$+\boldsymbol{Q}_2\delta\Big(x-\frac{\sqrt{3}}{2}R\Big)\delta\Big(y+\frac{R}{2}\Big)+\boldsymbol{Q}_3\delta(x)\delta(y-R)\Big\}\delta(z), \tag{54}$$

where $\boldsymbol{Q}_1=(-e/2, -e/2\sqrt{3})$, $\boldsymbol{Q}_2=(e/2, -e/2\sqrt{3})$ and $\boldsymbol{Q}_3=(0, e/\sqrt{3})$. The static baryon potential obtained is given as

$$V=\sigma\times(\text{minimum string length})-\frac{e^2}{24\pi}\sum_{i<k}\frac{e^{-mr_{ik}}}{r_{ik}}, \tag{55}$$

where the minimum string length is the minimum of the sum of the strings between static quarks. There are two types of the minimum configurations corresponding to the type of the three quark triangle. When all angles of the triangle are less than $\pi/3$, then the minimum configuration corresponds to three straight strings all angles between which are equal ($\pi/3$). If the angle at a quark is larger than $\pi/3$, then two straight strings between the quark and the others are the minimum configuration. See Fig. 8. It is stressed that the real three point interaction appears in the potential.

4.2.3. Meson-meson interaction

It hadron-hadron interactions are evaluated assuming two-body linear interactions between quarks and anti-quarks, a long-range Van der Waals force would appear between hadrons. But it is not consistent with experimental results. Let us study meson-meson interactions for the simplest two quark plus two anti-quark configuration in the framework of our model.[18] We introduced the following static currents:

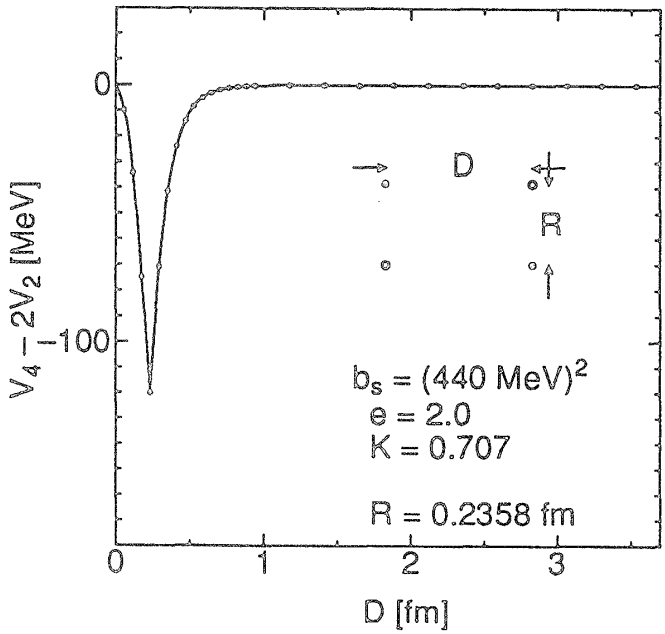

Fig. 9. Meson-meson interaction for the simplest configuration.

$$j^{\sigma}_{ex}=g^{\sigma 0}Q_1\left\{\delta(x)\delta\left(y-\frac{D}{2}\right)\delta\left(z-\frac{R}{2}\right)-\delta(x)\delta\left(y-\frac{D}{2}\right)\delta\left(z+\frac{R}{2}\right)\right.$$

$$\left.-\delta(x)\delta\left(y+\frac{D}{2}\right)\delta\left(z-\frac{R}{2}\right)+\delta(x)\delta\left(y+\frac{D}{2}\right)\delta\left(z+\frac{R}{2}\right)\right\}. \tag{56}$$

Solving the equations of motion with the static source, we evaluated the four point potential. Subtracting two times the quark-antiquark potential, we got the genuine meson-meson interaction as shown in Fig. 9. No long-range force between the mesons appears as expected. The interaction works only when both distances R and D are approximately equal. This is qualitatively in agreement with the string flip model[29] and the Monte Carlo results.[30]

4.2.4. Deconfinement transition in finite-temperature QCD

Confinement-deconfinement transition at finite temperature is investigated by evaluating the effective potential using the imaginary time formalism on the basis of the above infrared effective dual QCD model realizing quark confinement at zero temperature.[16]

Making the high temperature expansion and adopting terms of up to T^2 order, we obtain the effective potential $V_{\rm eff}$ in $SU(2)$ QCD:

$$V_{\rm eff}=-\lambda v^2\hat{\chi}^2+\frac{\lambda}{4}\hat{\chi}^4+\lambda v^4-\frac{\pi^2T^4}{15}+\frac{T^2}{24}\left\{4\lambda(\hat{\chi}^2-v^2)+3g^2\chi^2\right\}. \tag{57}$$

The vacuum expectation value $\langle\chi\rangle$ of the monopole field is determined by the relation

$$\left.\frac{\partial V_{\rm eff}}{\partial\hat{\chi}}\right|_{\hat{\chi}=\langle\chi\rangle}=\langle\chi\rangle\left\{-2\lambda v^2+\frac{T^2}{24}(8\lambda+6g^2)+\lambda\langle\chi\rangle^2\right\}=0. \tag{58}$$

Then

$$\langle\chi\rangle=\begin{cases}0\,, & T>T_c\,,\\ \sqrt{2v^2-(4+3g^2/\lambda)T^2/12}\,, & T<T_c\,,\end{cases}$$

where the critical temperature T_c is determined when the coefficient of $\hat{\chi}^2$ is zero:

$$T_c{}^2=\frac{24v^2}{4+3g^2/\lambda}\,. \tag{59}$$

The value of $\langle\chi\rangle$ disappears at $T=T_c$ continuously. The second-order phase transition occurs in the pure $SU(2)$ case in agreement with the Monte Carlo data.[31)]

In the infrared effective Lagrangian in pure $SU(3)$ QCD (48), we considered the simplest self-interactions of the monopole fields. But there are two other $U(1)\times U(1)$ invariant renormalizable interactions which we should consider in general. It is necessary to consider all types of possible interactions to study the order of the phase transition. Here the following self-interactions are discussed in place of those in (48):

$$\mu^2\sum_{\alpha=1}^{3}\chi_\alpha\chi_\alpha^*+\kappa(\chi_1\chi_2\chi_3+\chi_1^*\chi_2^*\chi_3^*)-\lambda_1(\sum_{\alpha=1}^{3}\chi_\alpha\chi_\alpha^*)^2-\lambda_2\sum_{\alpha=1}^{3}(\chi_\alpha\chi_\alpha^*)^2\,.$$

The final effective potential is

$$\begin{aligned}V_{\rm eff}=&\frac{1}{2}(\hat{\chi}_1{}^2+\hat{\chi}_2{}^2)\{\tilde{\mu}^2+T^2\tilde{g}^2\}+\frac{\tilde{\kappa}}{3}(\hat{\chi}_1^3-3\hat{\chi}_1\hat{\chi}_2{}^2)\\&+\frac{\tilde{\lambda}}{4}(\hat{\chi}_1{}^2+\hat{\chi}_2{}^2)^2-\frac{13\pi^2T^4}{90}+\frac{\mu^2T^2}{4}\,,\end{aligned} \tag{60}$$

$$\tilde{\mu}^2=3\frac{\mu^2}{2}\,,\qquad \tilde{g}^2=\frac{1}{8}(3g^2+8\lambda_1+4\lambda_2)\,,$$

$$\tilde{\kappa}=\frac{3}{\sqrt{2}}\kappa\,,\qquad \tilde{\lambda}=9\lambda_1+3\lambda_2\,.$$

Here we defined $\chi_\alpha=(\chi_{\alpha1}+i\chi_{\alpha2})/\sqrt{2}$ and make the shift $\chi_{\alpha i}\to\chi_{\alpha i}+\hat{\chi}_{\alpha i}$. Also we assumed that the symmetry under the discrete $2\pi/3$ rotation (Weyl symmetry) is not spontaneously broken:

$$\hat{\chi}_{11}=\hat{\chi}_{21}=\hat{\chi}_{31}\equiv\hat{\chi}_1\,,\quad \hat{\chi}_{12}=\hat{\chi}_{22}=\hat{\chi}_{32}\equiv\hat{\chi}_2\,.$$

The vacuum expectation values are determined by the following two relations:

$$\left.\frac{\partial V_{\rm eff}}{\partial\hat{\chi}_1}\right|_{\bar{\chi}=\langle\chi\rangle}=0\,,\quad \left.\frac{\partial V_{\rm eff}}{\partial\hat{\chi}_2}\right|_{\bar{\chi}=\langle\chi\rangle}=0\,. \tag{61}$$

They have three types of solutions that are transformed each other under the $Z(3)$ transformations in $(\langle\chi_1\rangle,\langle\chi_2\rangle)$ space. We analyse only the case $\langle\chi_2\rangle=0$. When $\langle\chi_2\rangle=0$, the vacuum expectation value $\langle\chi_1\rangle$ which gives the minimum potential is

$$\langle\chi_1\rangle=\begin{cases}0\,, & T>T_c\,,\\ \dfrac{-\tilde{\kappa}-\epsilon(\tilde{\kappa})\sqrt{\tilde{\kappa}^2-4\tilde{\lambda}(\tilde{\mu}^2+T^2\tilde{g}^2)}}{2\tilde{\lambda}}\,, & T<T_c\end{cases} \tag{62}$$

and

$$T_c=\frac{1}{\tilde{g}}\sqrt{\frac{\tilde{\kappa}^2}{9\lambda}-\tilde{\mu}^2}\ .$$

A typical first-order phase transition is seen. The infrared effective model reproduces successfully the behavior which is consistent with the Monte Carlo data.[31] The existence of the cubic interaction term is essential for the first-order transition.

§ 5. Conclusion and remarks

The idea that *monopole condensation is the color confinement mechanism* is very promising. All results of Monte Carlo simulations and the dual effective QCD model obtained so far are supporting the idea. It is remarked that the dual effective QCD model respects chiral symmetry keeping the confinement mechanism unaltered when two or three massless dynamical quarks are introduced. To study confinement and dynamical chiral symmetry breaking is very important.[32]

Acknowledgements

The author is thankful to Y. Matsubara, S. Kitahara, H. Shiba, S. Ejiri and O. Miyamura for collaboration and fruitful discussions. This work is financially supported by JSPS Grant-in Aid for Scientific Research (B) (No. 06452028).

References

1) G. t' Hooft, Nucl. Phys. **B190** (1981), 455.
2) T. Suzuki and I. Yotsuyanagi, Phys. Rev. **D42** (1990), 4257; Nucl. Phys. B (Proc. Suppl.) **20** (1991), 236.
3) T. Suzuki, Nucl. Phys. B (Proc. Suppl.) **30** (1993), 176 and references therein.
4) H. Shiba and T. Suzuki, Nucl. Phys. B (Proc. Suppl.) **34** (1994), 182.
5) H. Shiba and T. Suzuki, Phys. Lett. **B333** (1994), 461.
6) H. Shiba and T. Suzuki, Phys. Lett. **B343** (1995), 315.
7) H. Shiba and T. Suzuki, Phys. Lett. **B351** (1995), 519.
8) S. Ejiri, S. Kitahara, Y. Matsubara and T. Suzuki, Phys. Lett. **B343** (1995), 304.
9) S. Ejiri, S. Kitahara, Y. Matsubara and T. Suzuki, Nucl. Phys. B (Proc. Suppl.) **42** (1995), 481.
10) T. Suzuki et al., Phys. Lett. **B347** (1995), 375.
11) T. Suzuki and H. Shiba, Nucl. Phys. B (Proc. Suppl.) **42** (1995), 282.
12) Y. Matsubara et al., Nucl. Phys. B (Proc. Suppl.) **42** (1995), 529.
13) S. Kitahara et al., Prog. Theor. Phys. **93** (1995), 1.
14) T. Suzuki, Prog. Theor. Phys. **81** (1989), 752.
S. Maedan and T. Suzuki, Prog. Theor. Phys. **81** (1989), 229.
15) S. Maedan, Y. Matsubara and T. Suzuki, Prog. Theor. Phys. **84** (1990), 130.
16) H. Monden et al., Phys. Lett. **B294** (1992), 100.
17) S. Kamizawa et al., Nucl. Phys. **B389** (1993), 563.
18) H. Kodama et al., in preparation.
19) J. Arafune et al., J. Math. Phys. **16** (1975), 433.
20) T. A. DeGrand and D. Toussaint, Phys. Rev. **D22** (1980), 2478.
21) A. S. Kronfeld et al., Phys. Lett. **B198** (1987), 516.
A. S. Kronfeld et al., Nucl. Phys. **B293** (1987), 461.
22) J. Villain, J. Phys. (Paris) **36** (1975), 581.
23) T. L. Ivanenko et al., Phys. Lett. **B252** (1990), 631.
24) R. H. Swendsen, Phys. Rev. Lett. **52** (1984), 1165; Phys. Rev. **B30** (1984), 3866, 3875.

25) T. Banks et al., Nucl. Phys. **B129** (1977), 493.
26) J. Smit and A. J. van der Sijs, Nucl. Phys. **B355** (1991), 603.
27) S. Samuel, Nucl. Phys. **B154** (1979), 62.
28) M. Stone and P. R. Thomas, Phys. Rev. Lett. **41** (1978), 351.
29) K. Yazaki, Nucl. Phys. **A416** (1984), 87c.
30) A. M. Green et al., University of Helsinki Report HU-TFT-94-7 and LTH330, heplat/9404004.
31) For a review, see B. Svetitsky, Phys. Rep. **132** (1986), 1.
32) H. Suganuma et al., Report RIKEN-AF-NP-164.